Patterns and Acoustical Properties of Anomalous Environmental Sounds

Paul Dennis Sporer

Unusual sounds in the natural environment, variously described as unexplained detonations, Seneca guns, barisal guns, etc, have been reported by numerous credible witnesses around the world. The cause of these distinctive acoustical anomalies has been speculatively linked to weather or seismic factors, but due to the absence of 'hard data', scientific investigation into these events has not been forthcoming. Thus, there is no definitive knowledge about the mechanisms and processes behind the sounds. However, on October 6, 2011 in New York State, powerful evidence of this elusive auditory phenomenon was collected in the form of a high quality hour-long digital recording. Using original methodology, an extensive analysis of the recording was carried out in both the time and frequency domains, with the conclusion that highly systematic patterns of activity occurred during this event, indicating a well-ordered sound generating mechanism.

In the field of acoustics, many studies have given us a deeper understanding and appreciation of the inner workings of well-known sound generating mechanisms, such as the human voice, musical instruments, engines, etc. Notwithstanding these advances, there are very few investigations where the origin of the sound under study is unidentified, and no determinative process that reveals in detail the acoustical properties of unprovenanced phenomena has yet been formulated. However, reliable geographically wide-ranging accounts of what we term anomalous environmental sounds (AES) have been available for at least 200 years, clearly establishing a legitimate area of scientific interest. Witness reports describe AES as follows: In India, as a dull muffled boom as of distant cannon, called 'barisal guns';[1] in Italy, as longer than that of a cannon shot, though more prolonged and dull;[2] in Australia, as a dull roar increasing in loudness and then decreasing, likened to distant, prolonged peal of thunder or the discharge of a far-away piece of ordnance;[3] in Haiti, as thunder rolling in the distance, of dynamite exploding, or of cannon being fired off;[4] in Jamaica, as heavy fire of artillery;[5] in Western colonial America, as successive reports, resembling the discharge of several pieces of artillery, usually in calm weather;[6] in New York State around Lake Seneca as distant, muffled, repeated booming, like a far away cannon, called 'Seneca guns'.[7] There are also patterns reported. A British official in Bengal heard the sound of big guns in the distance, but the report was always double, as an echo. Further, they were always heard in triplets, and the interval between the three was usually three seconds, though in some cases it was up to ten seconds. They were heard most frequently from February to October. Interestingly, the official tried to move toward the sounds but was not able to get nearer to them.[8] Another report from Florida claimed that the sounds came at intervals of about five minutes.[9] Sometimes AES are tied to earthquakes. Before an earthquake on May 31, 1897 in Virginia, sounds like the explosion of distant artillery were heard, and people were disturbed by subterranean noises.[10]

The facts gathered from these and other AES reports provide the basis for a profile of the phenomenon: the sound is often a type of muffled boom; at least several sounds are heard during an event; usually there is no discernable pattern, but in a number of cases there is clear periodicity. Yet these reports also make clear why a determinative process of AES study is lacking: no event has yielded sufficient objective data for scientific analysis. However, a recent AES event in New York State has changed the situation. Due to diligent field research, an unprecedented amount of information was obtained, and we are able to present for the first time an effective procedure for AES study.

Circumstances of observation

AES of the general type described in the preceding section were detected in Chester, New York, USA, at Observation Point 1 (OP-1) beginning at 9:45am, Oct 6, 2011. A field recording was made of AES using a digital recorder that was set up at OP-1 above and away from any obstructions (See Methods). The nearest street intersection to OP-1 is located at N41° 22.207', W74° 16.831', altitude 585ft. During the event, observation of AES was also made at Observation Point-2 (OP-2), N41° 22.809', W74° 17.425', which is on a footpath called the Heritage Trail. Best estimate compass headings of 30°T from OP-1, and 42°T from OP-2 were obtained. Direct distance between OP-1 and OP-2 is 1.59 km. During the AES event, no earth tremors were felt, no unusual visual phenomena, odours, or animal movements were noticed. See Supplementary Fig 1 for a map and photos of the area.

The observation of the sounds was in the town of Chester, Orange County, 72km NW of New York City, 147km S of Albany. The 2010 county population was about 370,000, density of population 176 persons/sq km. The rural region is of moderate elevation, low hills, containing a mixture of single family homes, farmland, pasture, and forest. No large factories, military bases, or major airports are within 20km of OP-1.

We have seen that historically AES were sometimes linked to weather phenomena. Official records of nearest airport KMGJ showed that for the period 9am to 1pm of Oct 6, 2011, visibility was at 10 mi; sky clear; wind was mostly calm, with breezes up to 7mph and no gusts; direction of wind was SSW to WNW (200-290 deg); temperature rose 45°F to 65°F; relative humidity fell 82% to 29%; barometer fell 30.37in to 30.31in. Weather parameters for this day and for several days before and after the event were within normal ranges for the time of year, and there is no apparent connection to AES.

Certain reports link AES to seismic activity. An investigation showed that significant seismic events are rare in Orange County, as indeed they are for the Northeast. A search for epicentres in an

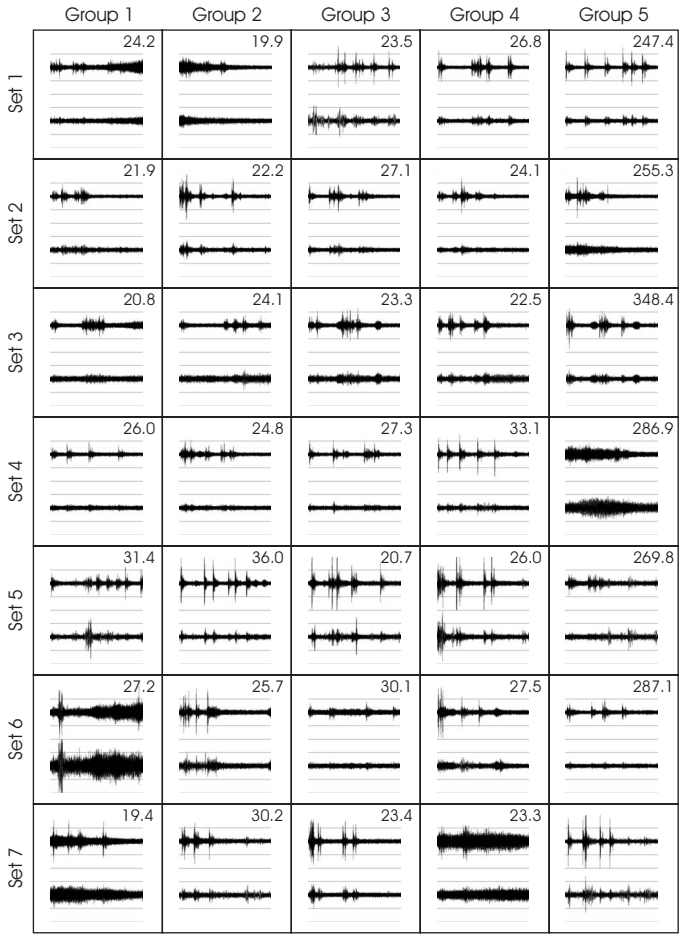

Figure 1. Table of AES waveforms in TD, segregated by group and set, with each cell showing stereo separation of raw data, left channel on top, right channel on bottom. The x-axis in each cell is Time (sec), and the y-axis is Amplitude (%), with 0% centre, 50% at intermediate lines, and 100% at top and bottom. Each graphic represents about 5s, and above this graphic in the corner is time in seconds to the next group.

area with a 70km radius from OP-1 revealed no events in 2011, and 7 events, magnitude 2.0 to 2.6, occurred Dec 26, 2009 to Dec 25, 2010; these were located mainly in northern New Jersey, and none near OP-1. A wider search of 300 km showed that in 2011 a series of earthquakes, magnitude 2.5 to 3.0, with epicentres in the Altamont, NY area, occurred Aug 23, 25, 26, 27.[11] Apparently, these events did not produce any seismic activity in the area around OP-1, but an Aug 23rd magnitude 5.8 earthquake centred near Richmond, Virginia, did create noticeable tremors (level IV intensity, Modified Mercalli) in Orange County.[12]

Thus, based on the evidence, no conventional phenomena were the direct cause of AES of Oct 6, 2011, although unconventional seismic activity in certain parts of New York State in late August might have been an indirect cause.

Audio analysis of AES

The recording of the event was first explored using hearing analysis (See Methods and Internet link below for sound files). The subjective impression was that the recording contained punctuated sounds of distinct tonal qualities not connected with anything known; AES possess certain attributes like those found in thunder, cannon fire, and fireworks, but AES are immediately distinguishable from conventional sounds. An appropriate descriptive term of the most prominent AES might be 'thud', since the low frequency (LF) sound has some force but appears muffled or dampened. We will also use the term 'rumble' to describe less prominent and even lower frequency content that is clearly associated temporally with the thud sounds.

Since the hearing of sound is a fleeting subjective impression, interpreted within a matter of less than one-half second, the use of computer tools can aid in analysis. Thus, graphic representations of time-domain (TD) based amplitude (AT) allow us to distinguish many detailed acoustical characteristics of AES. Specifically, an AES waveform has an 'attack' portion that leads to the first AT peak, the 'middle' portion after the first peak, consisting of undulations including further peaks, and the 'decay' portion after the last peak, which goes back to background state. We might look at the situation as the following: the normal acoustical 'state' for the countryside of upstate New York in early October is a combination of essential 'silence' (meaning no continuous sound except that coming from certain insects), and occasional known sounds emanating from people, birds, automobiles, trucks, aeroplanes, lawnmowers, helicopters, etc. This normal state is disrupted by sounds for which an origin, either manmade or natural, cannot be established. These sounds continue for a short period, after which AT goes back to normal background state (or silence). Thus, by isolating sounds of interest from non-important ones, we can determine that our recording contains over 140 unassignable sounds.

Based on this reasoning, we were able to organise AES using a partition scheme. In operational terms, we call each distinguishable sound an 'element': a number of nearly contiguous, distinct, closely related AT peaks. The time between elements clearly varies, with most occurring within only 1-2s of each other, but some elements are separated by much longer time. Thus, we can define a collection of elements as a 'group', which begins with the attack of the first element, and ends with an element not followed by another element within 5s. Further, it is clear that there is a long period of silence between certain groups, so we can bring together a number of groups into 'sets'. Hence, the individual sound units are delineated by periods of 'silence', short between the elements in a group, longer between groups, and then longest between the last group of a set, and the first element of the next set.

Fig 1 contains TD graphs created using our partition scheme (Methods), and it shows patterns of AES which are consistent and extensive. Thus, a number of elements make up a group, 5 groups make up a set, and 7 sets constitute the AES event. The thud elements always occur in the L channel, because of the way the recorder was pointed, along a generally north-south axis, with the sound coming from 30°T. The rumbles, usually heard on the R, were not counted at this time. There are 28 (7x4) groups of thuds, not counting the last group in each set, the mean time between groups of 25.517s, sd=4.197, se=0.793, min=19.440, max=37.827, p=0.000000, range of 18.387. There are 6 sets, with a mean time between of 282.484s, sd=36.103, se=14.739, min=247.373, max=348.413, p=0.000000, range of 101.040. The nomenclature we will use is that of Set and Group, so, S1G1 will mean Set 1, Group 1.

Further analysis of the intrinsic aspects of each group shows two general patterns of waveform distribution: one where they are fairly equally spaced, and another, where they are clustered. An interesting characteristic in respect to the latter, is that in cases where two or more similar waveforms are partially overlaid, they appear to the ear as a single sound with pseudo-reverberance.

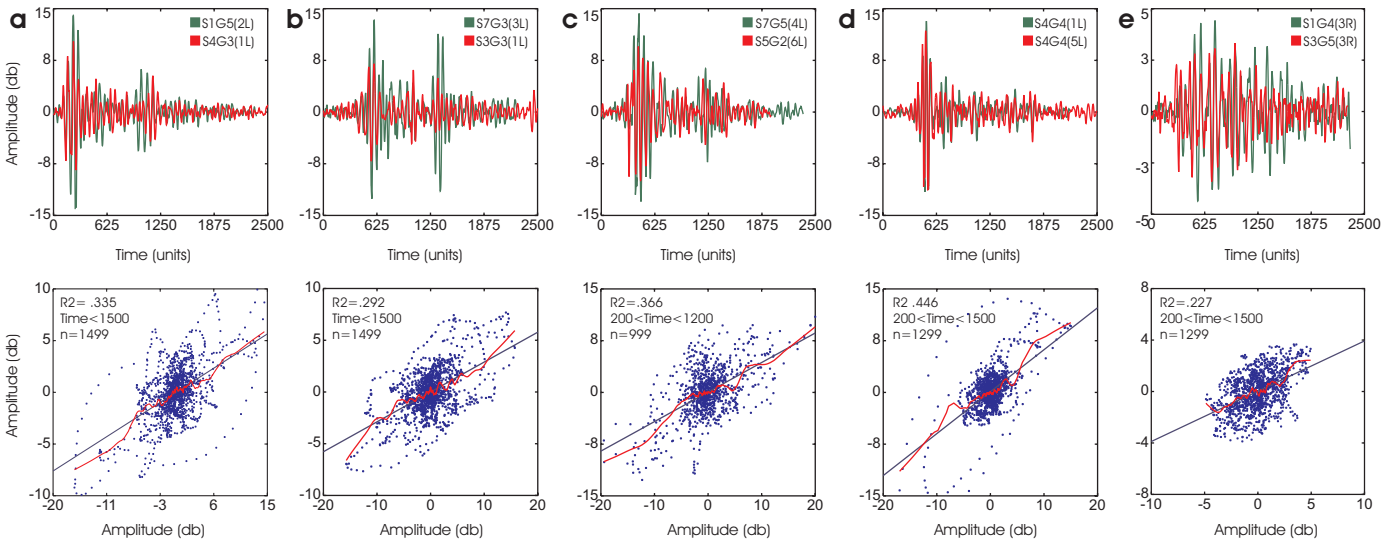

Figure 2. Graphs of TD data, showing correlations of elements. Top row has graphs with superimposition of two waveforms, Lowess smoothing (LS) of 20; x-axis has units equal to 0.159ms. Set and group are shown in top right corner, with position of element in group and recording channel in brackets. Bottom row shows filtered point data, with green variable on x-axis, red variable on y-axis. A simple regression line is superimposed; another red line LS of 100 is overlaid as well. S1G4 is also in Supp Fig 3a; S1G5 in Supp Fig 3b; S4G4 in Supp Fig 3g, Supp Fig 4d; S7G5 in Fig 3c.

An analysis was then carried out to determine the level of TD waveform correlations within and between groups. Using a correlation matrix (Methods), we found numerous instances of significant correlations between sound elements, showing extraordinary consistency within a natural phenomenon (see Supplementary Fig 2). Different aspects of internal properties are shown in selected higher correlation pairs of elements in Fig 2. The top row graph overlays exhibit precise construction, even where there are multiple peaks, or where the main peak arrives sooner. 2a, rapid attack, with a sharply defined main peak. 2b, slow attack, strong twin peaks, elements show correspondence at some 20 groups distance. 2c, moderate attack, longer middle portion. 2d, slow attack, single peak curve shows strong correlation within the group. 2e, R channel 'rumble', with slow attack, long middle portion, with multi-peak correspondence. Thus, even though elements can exhibit diverse characteristics, there is impressive agreement in the waveform details of unconditioned audio. The lower scatter plots further support the consistency principle, demonstrating a good directional aggregation array of points along the slope.

After discovering high consistency in the TD, we then examined the frequency domain by carrying out a three-dimensional analysis (Methods). Fig 3 and Supplementary Fig 3 display 3D graphs showing frequency spectrum (FS) development over time (see in conjunction with Fig 1). These graphs indicate similar sequences of well-defined, detailed, lateral profile 'waves'. The strongest peaks of AES signal are found in the 90-130hz range, with relatively smooth inclines on each side. There is significant activity all the way down to 30hz in the L channel, and even further down to 10hz in the R. Despite this subsonic component, no earth movement was felt during the event, and as we have seen, no earth tremors were recorded in the region. There is often a small but significant component from about 200hz to about 500hz, which gives the sound more presence. Although the large majority of thuds are from the same relative location on the stereo spectrum (found on L), there is the intriguing characteristic that on many occasions, the R channel produces a type of LF rumbling sound often in conjunction with a more 'typical' AES from the L. This is clearly seen in S5G5, where the rumbles are set 'in motion' after the thuds, with no activity preceding the group on either channel (Supplementary Fig 3j). In several instances there were 'precursors', meaning attenuated thuds that just preceded the main group, and where activity on the L sometimes interacts with the R. We see this in Fig 3a, wide broadband LF precursors on R, that abate during thuds on L. 3b, thuds on L give peculiar subjective impression of 'hammering', preceded

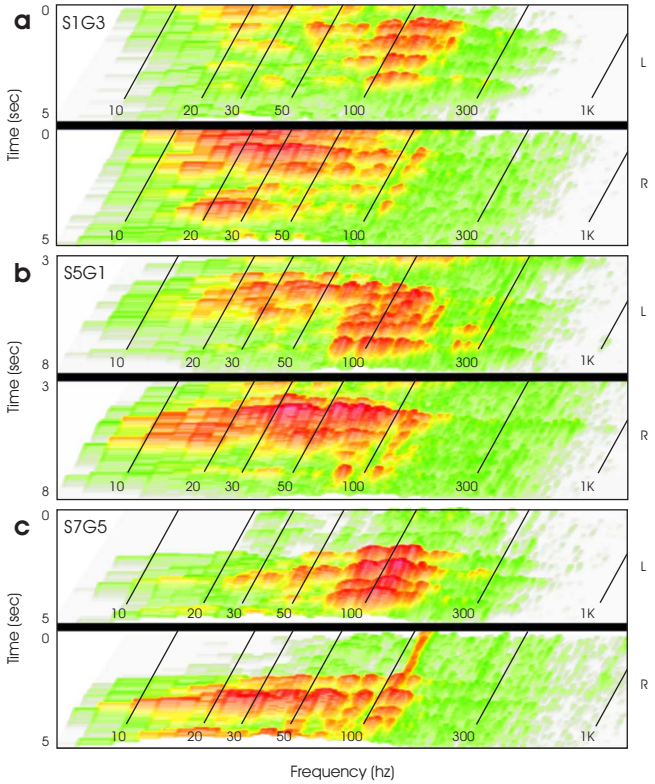

Figure 3. Three-dimensional graphs show x=frequency, y=time, z=amplitude (colours show increasing AT: green-yellow-orange-red) using raw audio data. Developmental patterns of frequencies over time, as well as the interplay of energy between L and R channels, is clearly visible. A specific element from S7G5 is in Fig 2c.

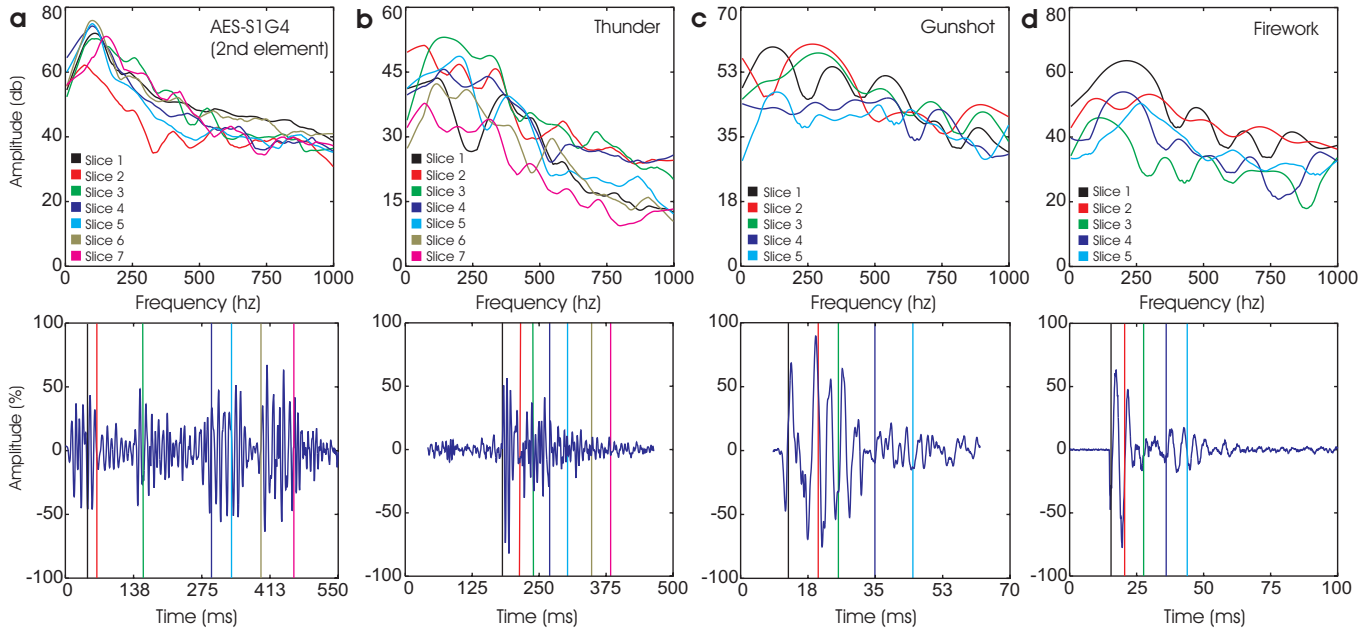

Figure 4. Comparison between FS of AES, thunder, gunshot, and firework, using time-sectional smoothed data overlays of each event. Top graphs are frequency domain based, showing colour-coded FS slices of each event, with LS of 50; amplitude is arbitrary value, with 0db as baseline. Bottom-row graphs show time domain curve where slices were taken from a sound element; vertical coloured lines indicate the beginning of the slice; slices proceed from L to R on the graph; AT is on a scale of +/-100%. The AES element can be seen in the 3D soundfield in Supplementary Fig 3a.

by strong rumbles on R. 3c, four evenly spaced thuds on L, with quieter precursors (green 'waves') that to an extent 'mimic' the succeeding thuds; broadband rumbles are in the middle of group.

Because of the consistency shown in the frequency domain, we further examined the extent of FS correlations (Methods). We took selected time sections from each group for comparison, created a correlation matrix, which exhibited numerous high correlations. Detailed inspection of selected FS presents good correspondence in details, establishing what appears to be a 'signature' of AES, where the subsidiary peaks are whole-number multiples of the main peak. Supplementary Fig 4a contains nine FS curves overlaid, showing a hypothetical fundamental of 126hz and six upper partials. There are clear consensus peaks for the fundamental and first three upper partials, which leads us to think that there are quasi-musical factors at work. Supplementary Fig 4b shows a one to many relationship exhibiting similar consistency. We can see that AES is not chaotic broadband, but a remarkably well-organised series of peaks, showing great correlation between elements belonging to different groups. Certain groups show FS peaks with apparent mathematical organisation, implying that there might be 'tones' (a fundamental plus upper partials) within the structure of AES. An examination was made of four FS for the presence of harmonics, with the result that the hypothesis of quasi-musical characteristics cannot be rejected (see Supplementary Fig 4c-f). Possible fundamentals are at about 75, 78, 95, 110, 114, 116, 127, 128, 130, 170, each with 5 or more upper partials present up to 1000hz. Although there is no apparent musical quality to AES, it is theoretically possible to create 'noise' by combining musical tones. Many of the groups show FS which contain possibly three or more 'tones' superimposed, where the fundamental and upper partials are shown as peaks. Although the upper partials are not exact multiples of the fundamental, it could be an indication of inharmonicity, which also occurs in certain musical instruments.

Thus, the AES sound generating mechanism (SGM) can produce a congruent interwoven texture, but the evidence so far does not give us complete understanding of the inner workings of the SGM. If AES are similar enough to a conventional sound, one with known properties, then this might help us construct a model of the SGM. Let us now compare AES to attributes of other types of sound that are reputed to have similar attributes: thunder, gunshots, and fireworks (Methods). Thunder is the result of a complex interaction of clouds, ground, and electricity. Following the lightning discharge, the heating of atmospheric gases around the channel cause a succession of compressions that are perceived as LF rumbling. However, manmade explosive products, such as gunshots or fireworks, use relatively simple chemical mechanisms to achieve a rapid blast, and so have short, punctuated elements peaking in the lower part of the FS. Results of our analysis are seen in Fig 4. The four types of sound showed markedly different properties. Despite the fact that the chosen AES element is one of the more intricate ones, each of the slices shows sharp well-defined peaks, as well as smaller subordinate 'parts' that vary in size. These features correspond well with each other across slices. Compared to AES, thunder also has defined peaks and smaller undulations, but little correspondence between slices. Gunshot and firework are very rapid phenomena, with simple, wider, rounded peaks, but with little correspondence between slices, especially in the main peak frequency area. An important factor is that, as frequency increases, only AES slices have a steady, smooth, more rapid slope down from the main peak. It is indisputable that AES show a distinctly higher order of spectral organisation, thus implying a 'refinement' that is missing in the 'primitive' mechanisms of the other three sounds. Our judgement is that we cannot use thunder or manmade explosives as guidance in constructing a model of the SGM of AES.

Discussion

After extensive analysis of the AES recording made on Oct 6, 2011, utilising specially designed acoustical, graphical, and statistical research methods, it is clear that we cannot assign these sounds to any known conventional category; indeed, their unique

character demands that they be put into their own category. When we bring together all of our results—compound periodicity (partitioning of sounds into groups and sets), correlations between TD waveforms, correlations between FS, negative correlations between intragroup L and R channel TD waveforms, pseudo-reverberance due to clustering of peaks, attenuated 'mimic' sounds that precede elements (precursors), associated infrasonic rumble component, and quasi-musical tonal qualities of elements—we reach the inescapable conclusion that AES are the product of a large-scale, highly developed, and solidly structured system. Hence, the AES observed in the Chester, NY event are extraordinary, not only due to their rare occurrence, but also because they constitute evidence of a sophisticated phenomenon containing within its structure mechanisms that operate according to precise mathematical principles, of an order unlike any that has heretofore been studied in Nature.

We believe that, due to the wealth of information that has been obtained, a productive line of enquiry has been successfully carried out, and moreover, a protocol of analysis has been established that can be used for further investigation. Now that the wider scientific community has been made aware of the characteristics of AES, it is hoped that more recordings will be analysed, as undoubtedly these events continue to occur in many places of the world.

METHODS

An audio recording lasting 57m 39s was made on Oct 6, 2011, starting at 9.45am EST, from OP-1, using a digital recorder, which was about 60m from the nearest road, and about 15m above the road surface. The device was placed in an area enclosed on three sides, to protect it from wind and stray sounds. The unit was not touched during recording, except at beginning and end. The orientation of the recording unit was on the 11 deg—191 deg axis, L channel to R channel. The recording unit has a reported frequency response of 50 to 19,000hz, although the actual response might be significantly under 50hz; the format was 16 bit, stereo, sample rate of 44.1k. For analysis, WAV files were used.

Three versions were used for analysis: An unenhanced 44.1k version (raw audio); an enhanced 44.1k version; and an unenhanced 6.3k (decimated) version. For the subjective listening analysis, the enhanced version was created using various conditioning methods. One method removes covering noises of a continuing, relatively invariant nature, without affecting the acoustical characteristics of the target sounds; a short sample of noise is used as the basis for the reduction algorithm. Another method involves a parametric EQ, set to remove about 10db at two frequency 'notches', with Q at 3 to 6. These tools facilitate the perception of the distinctive qualities of AES by allowing detailed nuances and subtleties to 'come through', without accentuating them. Using observations gained from subjective listening, a general protocol for the treatment of data was developed. Note that all statistical procedures utilised unenhanced raw recording data, meaning that the material was not conditioned in any way.

Partition of Data

Using the enhanced version of the recording, all AES were identified through hearing, and were also matched visually on the audio timeline. In this way, the exact temporal position of each sound could be verified. The AES groups and sets were then created using the method described in the text. Fig 1 table contains unenhanced audio TD waveforms obtained from the audio recording, with first significant deviation from background level marked as the beginning of a group. The distance of the first peak from the left side of the graph is a function of first attack (buildup of AT), which varies between groups. All graphs have AT on an arbitrary scale, with 100% set for the loudest sound of the entire event, all other sounds being scaled. Three groups show significant passing vehicles noise (S4G5, S6G1, S7G4), although the AES can still be identified.

Correlation matrix of TD waveforms

The table of figures in Supplementary Fig 2 was derived from a generated correlation matrix using TD data from all AES elements in the recording, which was decimated by a factor of 7. Figures are Pearson correlations, obtained using pairwise deletion, with significance for all pairs of p=0.000000. Figures are only shown if Pearson correlation was greater than 0.450. Cronbachs Alpha = 0.989; Standardised Cronbachs Alpha = 0.956.

Correlations of selected TD waveforms

Each graph in Fig 2 consists of two superimposed sound elements; an element can be seen as a cohesive unit of a main peak and subsidiary peaks. For the determining of correlations, raw audio material was decimated by a factor of 7. Data were filtered to remove random noise at the beginning and end of an element, thus largely limiting the focus of analysis to the central main part. All correlations have p=0.000000 for variable coefficient.

Three-dimensional analysis of FS

Graphs in Fig 3 and Supplementary Fig 3 had FS data derived from the raw audio data recording using the Fast Fourier Transform (FFT) procedure, with a sample size of 16384 points; thus, for a sample rate of 44100, there is a frequency limit of 22050, and spectral line resolution of 2.692. A Hanning Smoothing Window was used. The colour graphs were generated using a special visual optimisation procedure.

Correlations of FS

FS data from raw audio were obtained by, first, taking a 300-600ms section from the L channel of one element from each group; the element was chosen because it either was representative of that group, or contained the strongest, most developed waveform. The length of the section depended on the length and uniformity of the chosen element. No time filter was used. Second, each section was subjected to the FFT procedure, with an additional bin smoothing of 9. The resulting variables were then put into a correlation matrix, with significance for all pairs of p=0.000000. Pearson correlations for the large majority of pairs was greater than 0.800. Cronbachs Alpha = 0.981; Standardised Cronbachs Alpha = 0.943. From this table selections were made for display in the graphs in Supplementary Fig 4.

Comparisons of AES with other types of sounds

A comparison was made to determine the level of difference in FS attributes between AES, thunder, gunshot, and firework, with results shown in Fig 4. The four types were chosen because they approximately matched in terms of general loudness, tone, and duration. All four events were recorded with same recorder, and at the same position of OP-1. A recording of a passing Spring thunderstorm was made where several significant thunder elements occurred. A recording was made of gunshot sounds coming from rifles used by hunters in a nearby wooded area; the dis-

tance from the sound source to OP-1 was less than 0.5 km. A fireworks event in the area was recorded, where the products were of the professional variety, set off from about 1km away from OP-1; the element recorded was an aerial type bomb. For each recording, a representative element of sufficient clarity and AT was chosen. The second element from the S1G4 L channel was chosen as representative of the AES event. For each type of event, FS were obtained for 5 to 7 'slices' of time, as per FFT procedure, each slice ranging from 6 to 32ms in length, depending on the length of the element. The timeline position of the beginning of each slice was chosen randomly. The separate FS 'slices' can be compared within each type of sound and between types of sound. The bottom row of graphs show data decimated by 7 for AES, but no decimation was used for thunder, gunshot, or firework.

1. Scott, G. B. Barisal guns. *Nature* **53**, 197 (1896).
2. Anonymous. Oceanic and seismic noises. *Monthly Weather Review* **26**, 216 (1898).
3. Cleland, J. B. "Barisal guns" in western Australia. *Nature* **78**, 101-102 (1908).
4. Scherer, J. Notes on remarkable earthquake sounds in Haiti. *Seismological Society of America Bulletin* **2**, 230-232 (1912).
5. Templeton, E. C. Subterranean sounds heard in the West Indies. *Seismological Society of America Bulletin* **5**, 171-173 (1915).
6. Robinson, C. H. Barisal guns. *Nature* **53**, 487 (1896).
7. Anonymous. The "Guns" of Lake Seneca, N. Y. *Monthly Weather Review* **31**, 336l (1903).
8. Schurr, Henry S. Barisal guns. *Nature* **61**, 127-128 (1899).
9. Cooper, W. S. Barisal guns. *Scientific American* **75**, 123 (1896).
10. Bollinger, G. A. Virginia's two largest earthquakes. *Seismological Society of America Bulletin* **61**, 1033-1039, Aug (1971).
11. International Seismological Centre, On-line Bulletin, http://www.isc.ac.uk, Internatl. Seis. Cent., Thatcham, United Kingdom, 2010
12. USGS website, http://earthquake.usgs.gov/earthquakes/eqinthenews/2011/se082311a

Sound Files of the AES can be found at AnzaPublishing.com/AES.

Acknowledgments Special thanks to Cassandra Sporer for assistance in the preparation of this paper.

Author Information Correspondence and requests for materials should be addressed to paul_sporer@anzapublishing.com.

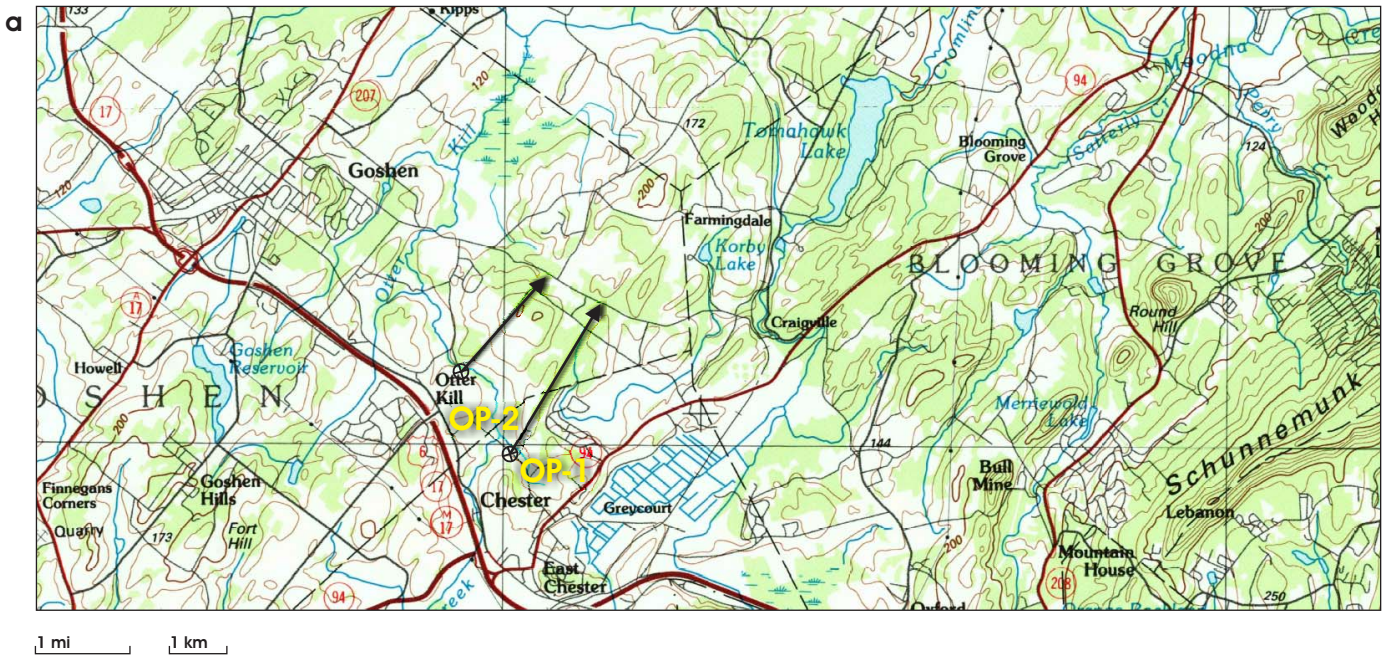

Supplementary Figure 1. Map and photos of Chester, New York area. **a,** map shows location of two observation points where compass readings were obtained. The convergence of lines from OP-1 and OP-2 should not be taken to mean that this point is the physical source of the AES. If the sounds originated from one distant point, they would emanate from only one part of the stereo spectrum in the recording, but since AES are not just present on the L, but also on the R, this implies that the origin is an area, not a point. Further research is required to determine the geolocation of the phenomenon. The map is a section taken from USGS geological survey 1986 map of Middletown, NY-NJ-PA, 41074-A1TM-100; scale 1:100,000; contour interval 20m. **b,** view towards northeast, showing traffic intersection marked OP-1 on above map, pointed in general direction of apparent AES origin. **c,** view towards northwest, in front of intersection, showing main road; apparent AES origin is to the right. Next photo was taken at top of rise ahead on main road. **d,** view looking north, on main road, with apparent AES origin to the right. The Heritage Trail is on the right just inside the wooded area. **e,** view looking east, at OP-2 on the Heritage Trail, with apparent AES origin to the left.

	Group 1	Group 2	Group 3	Group 4	Group 5
Set 1	S1G1(1R):S5G2(2R) (0.464) S1G1(2R):S5G2(1R) (0.489) S1G1(1L):S7G5(2L) (-0.518)		S1G3(2L):S7G3(2L) (-0.465)	S1G4(2L):S3G3(1L) (0.492) S1G4(3L):S3G5(3L) (0.539) S1G4(2R):S3G3(1R) (0.606) S1G4(2R):S5G2(3R) (0.504) S1G4(3R):S7G5(1R) (0.452) S1G4(3R):S3G5(3R) (0.569) **S1G4(2L):S1G4(2R) (-0.476)** S1G4(3L):S5G3(3R) (-0.525) S1G4(1R):S4G2(2R) (-0.473) S1G4(2R):S2G2(1R) (-0.457) S1G4(2R):S2G3(1R) (-0.589) S1G4(2R):S3G5(3R) (-0.526)	S1G5(2L):S4G3(1L) (0.542) S1G5(2R):S5G2(3R) (0.513) S1G5(1R):S2G2(1R) (-0.570) S1G5(1R):S2G3(2R) (-0.464) S1G5(1R):S5G2(4R) (-0.521)
Set 2	S2G1(1R):S3G3(1R) (0.451) S2G1(1L):S2G1(2L) (-0.510) **S2G1(1L):S2G1(1R) (-0.455)** S2G1(1L):S5G2(2R) (-0.581) S2G1(1L):S5G1(5R) (-0.450) S2G1(1L):S5G2(5R) (-0.573) S2G1(2L):S3G3(1L) (-0.485) **S2G1(2L):S2G1(2R) (-0.552)** S2G1(1R):S2G1(2R) (-0.450)	S2G2(1R):S5G2(4R) (0.500) **S2G2(1L):S2G2(1R) (-0.534)** **S2G2(2L):S2G2(2R) (-0.468)** S2G2(1R):S1G4(2R) (-0.457) S2G2(1R):S1G5(1R) (-0.579) S2G2(1R):S5G2(3R) (-0.498)	(1)		S2G5(1L):S4G4(4L) (0.496) S2G5(1L):S4G4(2L) (-0.582)
Set 3			S3G3(1L):S1G4(2L) (0.492) S3G3(1L):S7G3(3L) (0.553) S3G3(1R):S2G1(1R) (0.451) S3G3(1R):S3G5(1R) (0.462) S3G3(1R):S1G4(2R) (0.606) S3G3(1L):S2G1(2L) (-0.485)		S3G5(3L):S1G4(3L) (0.539) S3G5(1R):S3G3(1R) (0.462) S3G5(3R):S1G4(3R) (0.569) **S3G5(1L):S3G5(1R) (-0.510)** **S3G5(2L):S3G5(2R) (-0.485)** S3G5(3R):S1G4(2R) (-0.526)
Set 4		**S4G2(2L):S4G2(2R) (-0.544)** S4G2(2R):S1G4(1R) (-0.473) S4G2(2R):S4G4(5R) (-0.499)	S4G3(1L):S1G5(2L) (0.542) S4G3(3R):S7G3(2R) (0.465) S4G3(2L):S2G3(3L) (-0.460) **S4G3(2L):S4G3(2R) (-0.472)** S4G3(2R):S2G3(2R) (-0.478) S4G3(2R):S2G3(3R) (-0.521)	(2)	
Set 5	S5G1(6L):S5G3(3R) (0.451) S5G1(2R):S2G3(1R) (0.481) S5G1(1L):S6G4(2R) (-0.450) S5G1(2L):S5G2(3L) (-0.522) **S5G1(2L):S5G1(2R) (-0.508)** S5G1(5L):S4G4(2R) (-0.475) **S5G1(5L):S5G1(5R) (-0.470)** **S5G1(7L):S5G1(7R) (-0.489)** **S5G1(8L):S5G1(8R) (-0.466)** S5G1(2R):S2G3(1L) (-0.501) S5G1(2R):S5G2(3R) (-0.650) S5G1(5R):S2G1(1L) (-0.450)	(3)	S5G3(3L):S4G4(1L) (0.453) S5G3(3L):S7G5(4R) (0.455) S5G3(2R):S4G4(5R) (0.462) S5G3(3R):S5G1(6L) (0.451) **S5G3(3L):S5G3(3R) (-0.463)** S5G3(3R):S1G4(3L) (-0.525)		
Set 6		S6G2(2L):S6G4(2L) (-0.533)		**S6G4(1L):S6G4(1R) (-0.534)** S6G4(2L):S6G2(2L) (-0.533) **S6G4(2L):S6G4(2R) (-0.497)** **S6G4(3L):S6G4(3R) (-0.615)** S6G4(2R):S5G1(1L) (-0.450)	
Set 7			S7G3(3L):S3G3(1L) (0.553) S7G3(2R):S4G3(3R) (0.465) S7G3(2L):S1G3(2L) (-0.465) **S7G3(2L):S7G3(2R) (-0.518)**		S7G5(3L):S5G2(2R) (0.534) S7G5(3L):S5G2(5R) (0.547) S7G5(4L):S5G2(6L) (0.605) S7G5(1R):S1G4(3R) (0.452) S7G5(4R):S5G3(3L) (0.455) S7G5(4R):S5G2(6R) (0.562) S7G5(2L):S1G1(1L) (-0.518) **S7G5(3L):S7G5(3R) (-0.554)**

(1)

S2G3(1L):S5G2(3R) (0.456)
S2G3(1R):S5G1(2R) (0.481)
S2G3(2R):S4G4(2R) (0.455)
S2G3(1L):S2G3(1R) (-0.515)
S2G3(1L):S5G1(2R) (-0.501)
S2G3(2L):S2G3(1R) (-0.474)
S2G3(2L):S2G3(2R) (-0.562)
S2G3(3L):S4G3(2L) (-0.460)
S2G3(3L):S5G2(1R) (-0.483)
S2G3(1R):S1G4(2R) (-0.589)
S2G3(1R):S5G2(3R) (-0.469)
S2G3(2R):S1G5(1R) (-0.464)
S2G3(2R):S4G3(2R) (-0.478)
S2G3(3R):S4G3(2R) (-0.521)

(2)

S4G4(1L):S4G4(5L) (0.685)
S4G4(1L):S5G3(3L) (0.453)
S4G4(4L):S2G5(1L) (0.496)
S4G4(1R):S4G4(5R) (0.533)
S4G4(2R):S2G3(2R) (0.455)
S4G4(5R):S5G3(2R) (0.462)
S4G4(1L):S4G4(1R) (-0.486)
S4G4(2L):S2G5(1L) (-0.582)
S4G4(2L):S4G4(4L) (-0.496)
S4G4(2L):S4G4(2R) (-0.588)
S4G4(3L):S5G2(1L) (-0.531)
S4G4(4L):S4G4(4R) (-0.458)
S4G4(5L):S4G4(1R) (-0.541)
S4G4(2R):S5G1(5L) (-0.475)
S4G4(3R):S5G2(1R) (-0.502)
S4G4(3R):S5G2(2R) (-0.526)
S4G4(5R):S4G2(2R) (-0.499)

(3)

S5G2(2L):S5G2(5L) (0.636)
S5G2(6L):S7G5(4L) (0.605)
S5G2(1R):S1G1(2R) (0.489)
S5G2(1R):S5G2(2R) (0.463)
S5G2(2R):S7G5(3L) (0.534)
S5G2(2R):S1G1(1R) (0.464)
S5G2(2R):S5G2(5R) (0.809)
S5G2(3R):S2G3(1L) (0.456)
S5G2(3R):S1G4(2R) (0.504)
S5G2(3R):S1G5(2R) (0.513)
S5G2(4R):S2G2(1R) (0.500)
S5G2(5R):S7G5(3L) (0.547)
S5G2(6R):S7G5(4R) (0.562)
S5G2(1L):S4G4(3L) (-0.531)
S5G2(1L):S5G2(1R) (-0.484)
S5G2(2L):S5G2(2R) (-0.453)
S5G2(3L):S5G1(2L) (-0.522)
S5G2(3L):S5G2(4L) (-0.623)
S5G2(3L):S5G2(3R) (-0.481)
S5G2(5L):S5G2(5R) (-0.525)
S5G2(1R):S2G3(3L) (-0.483)
S5G2(1R):S4G4(3R) (-0.502)
S5G2(2R):S2G1(1L) (-0.581)
S5G2(2R):S4G4(3R) (-0.526)
S5G2(3R):S2G2(1R) (-0.498)
S5G2(3R):S2G3(1R) (-0.469)
S5G2(3R):S5G1(2R) (-0.650)
S5G2(3R):S5G2(4R) (-0.575)
S5G2(4R):S1G5(1R) (-0.521)
S5G2(5R):S2G1(1L) (-0.573)

Supplementary Figure 2. Table of within group and between group higher Pearson correlations of AES TD waveforms. The cell contains a list of group pairs, using nomenclature as shown in following example: S5G3(3L) means Set 5, Group 3, 3rd element, L channel. The number in brackets after the pair of groups is the correlation. The correlations were obtained using the filter 200<Time<1200, where the Time unit is equal to 0.159ms; resulting n=999. The numbers (1), (2), and (3) in the table indicate cells where the number of correlations was too many to fit, thus they are placed to the side. Bold type shows cases where a negative correlation implies that L and R channel elements are out of phase with each other. We can see here in the strong correlation of elements a remarkable consistency of the AES system, as was already evident in the phenomenon's significant periodicity (see Fig 1). With higher correlation, one might hypothesise that the sound comes from a stable process consisting of relatively few components in relatively simple configuration; assuming a certain probability that any one component will change over time, a mechanism with fewer components is more likely to be stable than one with many components. Further research is necessary to determine the validity of this hypothesis.

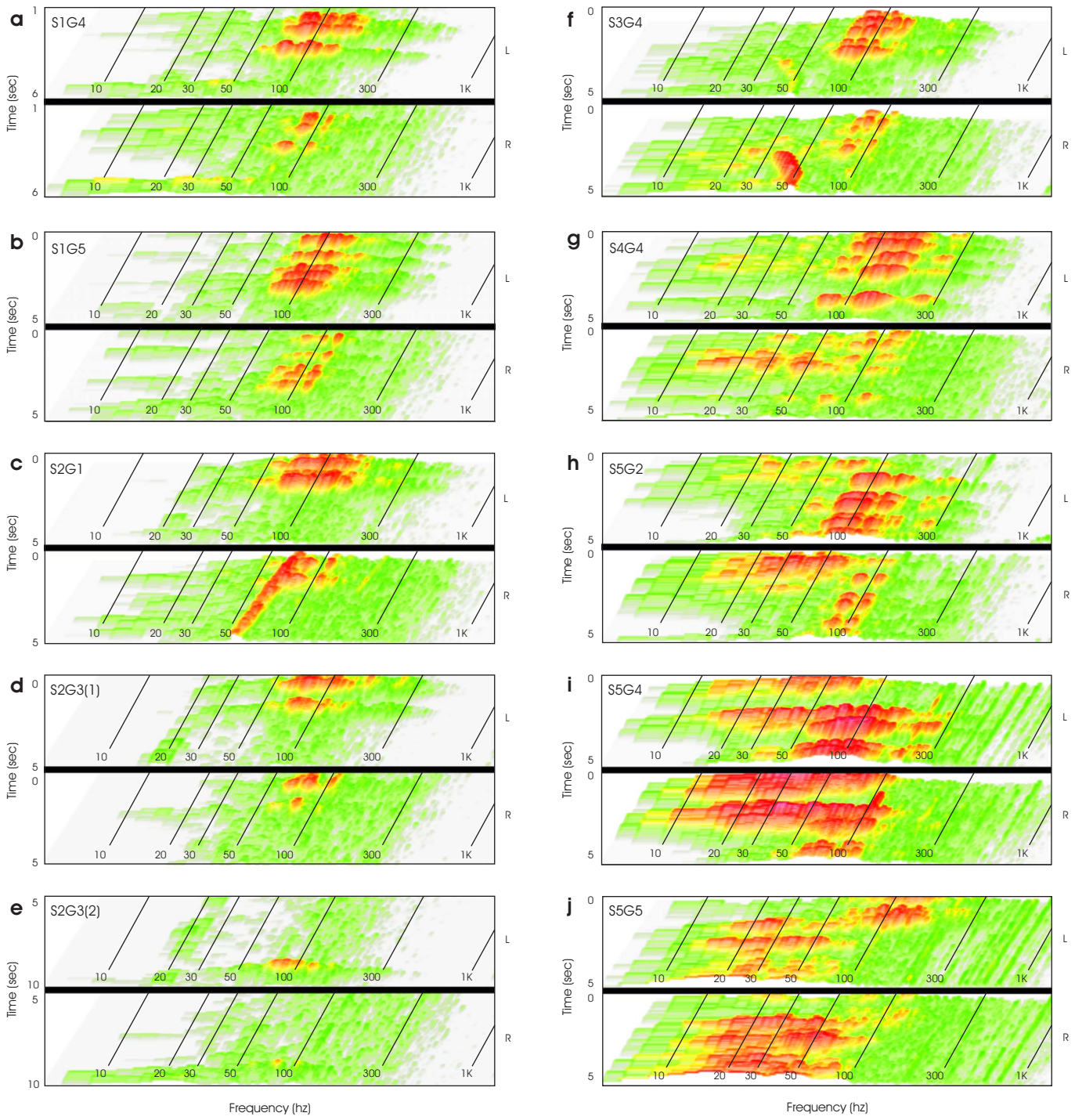

Supplementary Figure 3. Three dimensional graphs (frequency x time x amplitude), provide insight into the consistency as well as diversity of SGM, as well as possible modifications of patterns from beginning to end of whole event. Specific events from S1G5, S4G4 and S5G2 are seen in Fig 2a, d, c, and specific events from S1G4 are seen in Fig 2e and Fig 4a. **a**, graph begins with second element which is complex; no other significant activity in group, thus soundfield is fairly clean. **b**, the auditory perception here is that there is "reverberation", yet this effect is not from acoustical reflection, but from the SGM itself; the effect is due to a strong secondary peak for each thud (see Fig 1); group is remarkably clear of any material not related to main peaks. **c**, thuds are closer-spaced and varied in AT in TD, and they cover larger FS range; there is a peculiar band following the thuds at 60hz to 70hz, and proceeds about 12s in group before it ends. **d**, two thuds shown are actually each a collection of 3 rapid peaks in TD (see Fig 1); a well-formed narrow LF band at 22.95hz starts about 3sec before this group and continues on to **e**, and ends with final delayed thud on L; due to the LF position, this band can be felt more than heard. **f**, five evenly spaced thuds, with increased rumble activity on R; the strong curved red segment at bottom on the R is a vehicle driving off. **g**, five broader thuds shown, each with sharply-defined AT in TD, increasing AT first to last, as well as increasing spacing between; R shows broad rumbles in middle of group. **h**, clear broad LF precursors mainly on R, followed by clear even thuds, with sharply-defined AT in TD; however, after precursors, there is no LF activity on R. **i**, LF precursors, on both L and R, then four thuds with sharp multi-peak AT in TD; LF activity here is very broad, reaching far down into FS; peculiar, straight solid "spur" on R mid-field, at about 120hz. **j**, after 5 weakly defined thuds, continuous waves of broad low AT rumbles are set in motion after thuds.

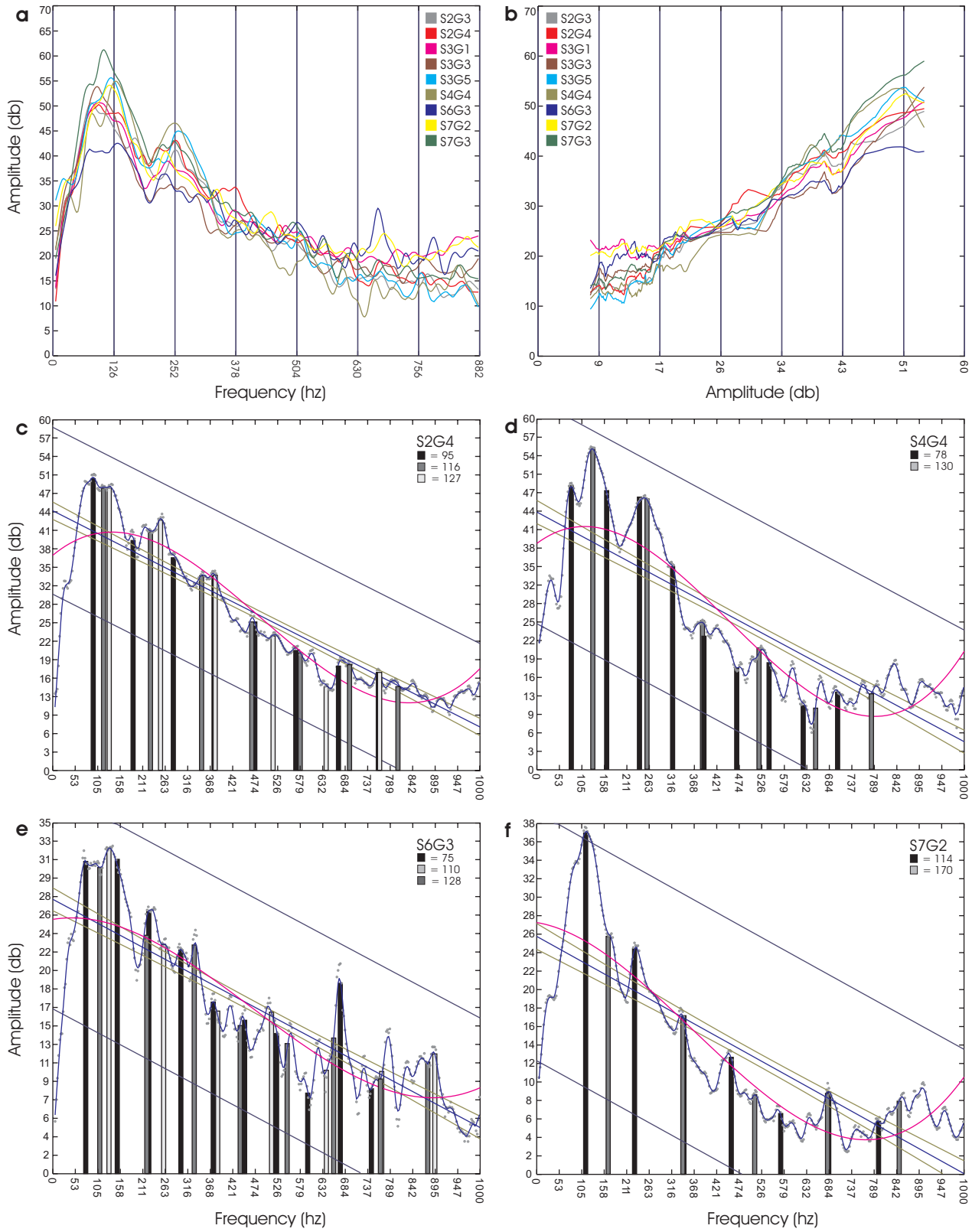

Supplementary Figure 4. Graphs showing different aspects of frequency spectra of AES events; all data are from L channel. S4G4 is also seen in Fig 2d, and Supplementary Fig 3g. **a**, FS overlays from different groups spread across whole event; LS of 11. Overlay graphs show consistency in FS distribution, with high detailed correspondence of peaks. **b**, groups from **a** plotted against S5G2, chosen because of high number of correlations with other groups in TD; LS of 20. This is further evidence of high correspondence between FS. **c-f**, details of four selected FS. Graphs shows thin blue FS curve, with LS of 10; thick blue line shows regression, least square line of best fit; inner gold lines show confidence level for the means; outer black lines show confidence level for individual points, alpha=.01; a purple line shows the third order polynomial fit over the data. Coloured bars represent possible fundamental and harmonics (ie, multiples of the fundamental; bars are not actual partials). The height of the bar is the approximate level of the harmonic. All graphs in this Figure show AT on an arbitrary scale.